
INVERSE THEORY

OPTIMIZED HIV DRUG TREATMENT USING PROBABILISTIC INVERSION

1 The Model for a Personalized HIV Treatment

In this section, we introduce a mathematical model that allows us to simulate the evolution of an HIV infection. After further investigating this model and discussing the impact of antiretroviral drugs, the optimal control problem is formulated.

1.1 The Dynamic Model

Since HIV was first simulated in the mid-90s, a wide variety of different models arose. Initially, they attempted to investigate the HIV evolution by a set of linear *ordinary differential equations* (ODEs). These, however, are only applicable for a short period of time, ranging in the orders of days. HIV, treated or untreated, is a disease that lasts for years, and accurate and reliable long-term investigations require non-linear models [1].

In addition hereto, the final model definition is determined by the choice of biological compartments and interactions that one wants to simulate. Some models, for instance, differentiate between potential target cells, usually including CD4+ T cells and macrophages [3]. Once a cell is infected, it can either remain in a latent state or actively reproduce new viral cells, causing different reactions of the patient's immune system [2].

A simple model, for instance, is shown in figure 1a. It describes the evolution of an HIV infection, assuming that no therapy measures are taken. However, to optimize HAARTs, we have to further evolve this model in order to not only simulate the interaction between viral and immune cells but to also consider the effect of drugs. For this, we first have to review the working principle and impact of HAART. Generally, this therapy is a combination of multiple classes of antiretroviral drugs, each fighting the virus in different ways. Two of these are *reverse transcriptase inhibitors* (RTIs) and *protease inhibitors* (PIs). While the first aims at blocking the initial infection of target cells, the latter causes already infected cells to only produce immature virus. Both these drugs, are solely designed for virus cells with a specific genome. HIV, however, replicates in untreated persons at an exponential rate, generating up to 10^{10} new free virus cells per day. Essential steps in this duplication are error-prone and hence, the probability of mutations is high. The emerging cells have modified genomes, and the deployed drugs inhibit them less efficiently. Thus, an appropriate model has to distinguish between drug-sensitive and resistant viruses [5]. Such a model is shown in figure 1b.

According to Rong et al. [5], the dynamics in figure 1b can be described by the following set of differential equations:

$$\begin{aligned}
 \dot{T}(t) &= \lambda - \gamma T(t) - k_s(1 - \varepsilon_{RT}^s)V_s(t)T(t) - k_r(1 - \varepsilon_{RT}^r)V_r(t)T(t), \\
 \dot{T}_s(t) &= (1 - u)k_s(1 - \varepsilon_{RT}^s)V_s(t)T(t) - \delta T_s(t), \\
 \dot{V}_s(t) &= N_s\delta(1 - \varepsilon_{PI}^s)T_s(t) - cV_s(t), \\
 \dot{T}_r(t) &= uk_s(1 - \varepsilon_{RT}^s)V_s(t)T(t) + k_r(1 - \varepsilon_{RT}^r)V_r(t)T(t) - \delta T_r(t), \\
 \dot{V}_r(t) &= N_r(1 - \varepsilon_{PI}^r)\delta T_r(t) - cV_r(t).
 \end{aligned} \tag{1}$$

Here, $T(t)$ denotes the concentration of uninfected target cells. Generally, by index s we denote the drug-sensitive strain whereas index r marks the drug-resistant one. Thus, $T_s(t)$ is the concentration of cells that

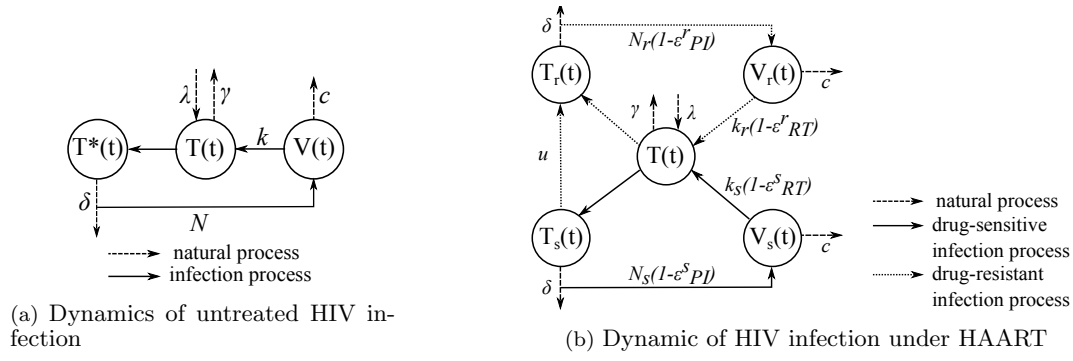


Figure 1: The above diagrams visualise two scenarios of an HIV infection. Model (a) describes the evolution of an untreated infection by distinguishing between uninfected target cells $T(t)$, infected ones $T^*(t)$ and viral cells $V(t)$. A healthy body strives to maintain a constantly high number of CD4+ T cells. While these cells die at the end of their life span with frequency γ , the human immune system continuously produces new ones at a birth rate λ . However, under the impact of HIV, the number of immune cells $T(t)$ is not only reduced by natural death but also due to the virus. First, CD4+ T cells are infected at rate k and the viral genetic material is included in their cellular DNA. During the remaining life time, the infected cell replicates the viral genes until it finally bursts, described by the bursting rate δ , and releases N new viral cells. Some of these, again, start infecting healthy CD4+ T cells while the rest die before they find a host cell which they can exploit to multiply their viral genes. Parameter c describes the death rate of viral cells. Opposed to that, model (b) explains the dynamics of a treated HIV infection, taking arising drug-resistant virus mutations into account. Although, the principle of the infection cycle remains the same, the extended model now differentiates between two cocirculating populations of cells: the ones which are susceptible to drugs, i.e. $V_s(t)$ and $T_s(t)$ as well as those that aren't, described by $V_r(t)$ and $T_r(t)$. Drug-resistant virus cells lead to infected cells which solely reproduce further resistant viruses. In contrast hereto, in a CD4+ T cell which is infected by a drug-sensitive virus, the HIV genome might mutate during replication and becomes resistant. Additionally, the diagram illustrates the effect of HAARTs. Tabel 1 summarises the meaning of the used parameters.

are infected by drug-sensitive viral cells $V_s(t)$, whereas $T_r(t)$ is the concentration of cells that are infected by drug-resistant viral cells $V_r(t)$. All concentrations are given in $1/ml$. Note, that the five compartments in model 1 are not directly observable in clinical data. Instead, blood measurements only give insight into the total viral load, i.e. $V_{tot}(t) = V_r(t) + V_s(t)$ and the overall number of immune cells, given as $T_{tot}(t) = T(t) + T_r(t) + T_s(t)$. Further, λ represents the birth rate of uninfected T cells per day, γ is their per capita daily death rate. The constant rates k_s and k_r describe how fast uninfected cells are infected by drug-sensitive and resistant virus, respectively. At the same time, these rates are reduced by the use of RTIs. The efficacy of the drug is given by the dimensionless parameters ε_{RT}^s and ε_{RT}^r , both ranging between 0 and 1. Since sensitive viruses are more susceptible to drugs, $\varepsilon_{RT}^s > \varepsilon_{RT}^r$. We assume that both kinds of infected cells, $T_s(t)$ and $T_r(t)$, burst and consequently die at the same daily rate δ . For sensitive virus cells, the number of released virus cells is denoted by N_s while N_r describes the same quantity in the drug-resistant case. However, under the deployment of PIs, not all of the newly generated free virus cells are themselves capable of infecting healthy immune cells. This is encoded in the efficacy parameters ε_{PI}^s and ε_{PI}^r . Again, $0 \leq \varepsilon_{PI}^s \leq 1$, $0 \leq \varepsilon_{PI}^r \leq 1$ and $\varepsilon_{PI}^s > \varepsilon_{PI}^r$. Virus cell populations are only reduced by their daily clearance rate c .

With the parameters ε_{RT} and ε_{PI} , we describe the efficacy of the single antiretroviral drugs. Summarizing these to the overall drug efficacy $\varepsilon = 1 - (1 - \varepsilon_{RT})(1 - \varepsilon_{PI})$ allows us to assess the efficacy of the combination therapy. Hence,

$$\begin{aligned}\varepsilon_s &= 1 - (1 - \varepsilon_{RT}^s)(1 - \varepsilon_{PI}^s), \\ \varepsilon_r &= 1 - (1 - \varepsilon_{RT}^r)(1 - \varepsilon_{PI}^r).\end{aligned}\tag{2}$$

Drug efficacy ε_s only depends on the current therapy and can directly be derived from drug dosages and intake durations. At the same time, we assume that the resistance level of the HIV mutants can be quantified by the parameter α ($0 < \alpha < 1$), which represents the reduction in drug effectiveness by $\varepsilon_{RT}^s = \alpha \varepsilon_{RT}^r$ and $\varepsilon_{PI}^s = \alpha \varepsilon_{PI}^r$. Additionally, the rate at which $T_s(t)$ cells become drug-resistant during the process of replication is given by the parameter u ($0 \leq u < 1$). In this chapter, we assume mild mutations, i.e. they appear rather seldomly and if they do, their susceptibility is only little reduced. Mathematically, this behaviour is achieved by setting $u = 3 \times 10^{-5}$ and $\alpha = 0.2$. With that, the constant efficacy parameters in relation 2 are known.

Parameter	Value	Description
λ	$10^4 \text{ ml}^{-1} \text{ day}^{-1}$ (estimated)	Birth rate of uninfected cells
γ	0.01 day^{-1} (estimated)	Natural death rate of uninfected cells
k_s	$2.4 \times 10^{-8} \text{ ml day}^{-1}$ (estimated)	Infection rate of target cells by drug-sensitive virus
k_r	$2.0 \times 10^{-8} \text{ ml day}^{-1}$ (estimated)	Infection rate of target cells by drug-resistant virus
u	3×10^{-5} (given)	Mutation rate from sensitive to resistant strain
δ	1 day^{-1} (estimated)	Death rate of infected cells
N_s	3000 (estimated)	Burst size of drug-sensitive strain
N_r	2000 (estimated)	Burst size of drug-resistant strain
c	23 day^{-1} (estimated)	Clearance rate of free virus
ε_{RT}^s	varies (given)	Efficacy of RTIs for sensitive strain
ε_{RT}^r	varies (given)	Efficacy of RTIs for resistant strain
ε_{PI}^s	varies (given)	Efficacy of PIs for sensitive strain
ε_{PI}^r	varies (given)	Efficacy of PIs for resistant strain
ε_s	varies (given)	Overall drug efficacy for sensitive strain
ε_r	varies (given)	Overall drug efficacy for resistant strain
α	varies (given)	Resistance level of mutant strain

Table 1: The tabel gives an overview about the model parameters, their definitions and physical units. The listed values, which are used for the numerical simulations to investigate the model, are based on a paper by Rong et al. [5].

Opposed to that, the remaining parameters, summarized in $\mathbf{m} = \{\lambda, \gamma, k_s, k_r, N_s, N_r, \delta, c\}$, strongly depend on the patient. However, with the given information about the therapy, they can be estimated from blood measurements. Descriptions and units of all parameters are summarized in table 1.

Before tailoring the above model 1 to a specific patient, its dynamic and steady state behaviour is validated by comparing numerical results to clinical observations and findings from research. In addition hereto, such simulations give deeper insight into the impact of antiretroviral drugs. If not stated differently, parameters are taken from table 1.

Firstly, we consider a pretreatment situtaion. A patient, who has been healthy until the very day of infection, has a CD4+ T cell count of $T(0) = 10^6 \text{ ml}^{-1}$. If she or he is infected by a viral load of $V_s(0) = 10^{-6} \text{ ml}^{-1}$, the untreated virus (i.e. $\varepsilon_s = \varepsilon_r = 0$) evolves within the first weeks as depicted in figure 2. Note, that although the transmitted pathogens could have already been mutated, it is assumed that $V_r(0) = 0 \text{ ml}^{-1}$. The further inital values are set to 0 [3].

From figure 2 it can be seen, that the dynamic characteristics of the model coincide with the previously described stages of an untreated HIV infection. While in the first few weeks, the viral load increases strongly, the number of uninfected T cells collapses, resulting in often observed flu-like symptomes. Following this, the model shows how the state of clinical latency sets in. Here, the viral loads as well as T settle in a steady state. Figure 2b demonstrates that without medication, the drug-sensitive strain dominates the infection throughout the considered time interval.

We assume that at this point of the disease, the infection is recognized and HAART is prescribed. With a presumed low resistance level of $\alpha = 0.2$, the therapy is quantified by $\varepsilon_{RT}^s = 0.4$ and $\varepsilon_{PI}^s = \varepsilon_{PI}^r = 0$. As initial values, the steady states of the pretreatment simualtion are chosen.

The numerical results, given in figure 3, show that indeed the therapy lowers the viral load and allows the number of uninfected immune cells to rise again.

An essential feature of the model is the development of the steady states as a function of medication efficacy of the drug-sensitive strain. This is demonstrated in figure 4, where the CD4+ T cell and viral count are plotted over ε_s . From diagram 4a, it can be seen that for low values of ε_s , HAART achieve an increase in the number of uninfected target cells. However, above a certain point, this growth saturates and the concentration remains on a constantly high level. We denote this point of maximal efficacy by $\varepsilon_{s,max}$. For the given set of model parameters, its value is $\varepsilon_{s,max} \approx 0.5$. A similar behaviour can be observed on the virus side, shown in figure 4b.

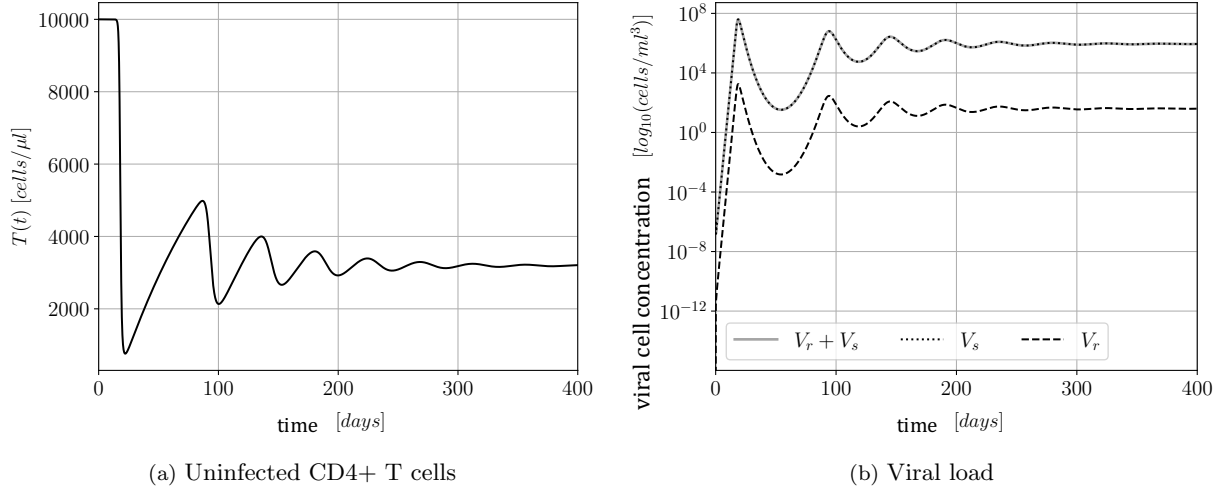


Figure 2: Simulation of the pretreatment evolution of an initial HIV infection. For the initial state, the following values are assumed: $T(0) = 10^6 \text{ ml}^{-1}$, $T_s(0) = 0 \text{ ml}^{-1}$, $T_r(0) = 0 \text{ ml}^{-1}$, $V_s(0) = 10^{-6} \text{ ml}^{-1}$ and $V_r(0) = 0 \text{ ml}^{-1}$ [3]. Diagram (a) describes the evolution of the uninfected CD4+ T cells during the first year. After an initial break-in of $T(t)$, which is followed by oscillations, the immune cell concentration finally settles at a low level. At the same time, the total number of viral cells, i.e. $V_r(t) + V_s(t)$ increases. This behaviour is shown in figure (b), where the concentrations of the total viral load as well as its two strains $V_r(t)$ and $V_s(t)$, is plotted in a semi-logarithmic scale. Similar to the immune cells, the concentrations of the virus exhibits oscillations, before it remains roughly constant.

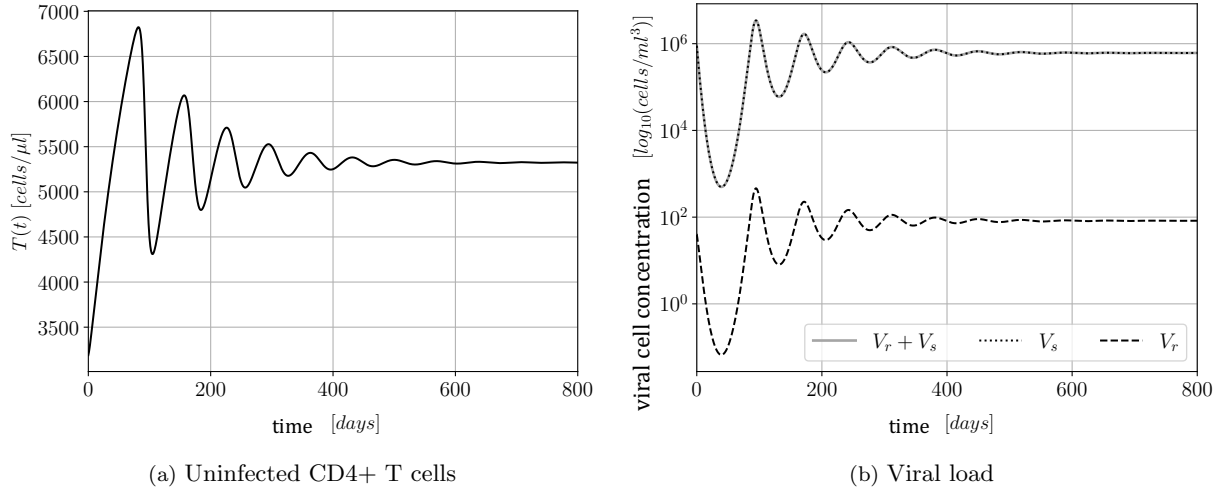


Figure 3: Simulation of the evolution of an HIV infection under HAART. It is $\varepsilon_{RT}^s = 0.4$, $\varepsilon_{RT}^r = \alpha \varepsilon_{RT}^s$ with $\alpha = 0.2$ and $\varepsilon_{PI}^s = \varepsilon_{PI}^r = 0$. The steady states of the preceding pretreatment simulation are used as initial values, i.e. $T(0) = 3.19 \times 10^5 \text{ ml}^{-1}$, $T_s(0) = 6.81 \times 10^3 \text{ ml}^{-1}$, $T_r(0) = 0.46 \text{ ml}^{-1}$, $V_s(0) = 8.88 \times 10^5 \text{ ml}^{-1}$ and $V_r(0) = 39.95 \text{ ml}^{-1}$ [3]. Diagram (a) shows the evolution of the CD4+ T cell count during the first two years of therapy. Similar can be seen in diagram (b), where the concentration of the viral load is depicted on a semi-logarithmic scale. Immune and viral cells are in a constant competition. Initially, therapy suppresses the reproduction of viral cells and hence, their concentration rapidly sinks. Consequently, more uninfected T cells are produced and $T(t)$ peaks in that first therapy phase. At the same time, this increased number of potential host cells for the virus again fuels its replication, resulting in a growth of $V_r(t)$ and $V_s(t)$. Figure (a) and (b) exhibit this interplay in form of oscillations. With time, this interaction diminishes and the concentration of immune and viral cells remain roughly constant. Further, figure (b) gives insight into the behaviour of the two viral strains. Since we are assuming mild mutations which occur seldomly which are still sensitive towards the drugs, the concentration of the drug resistant virus is remarkably smaller than $V_s(t)$.

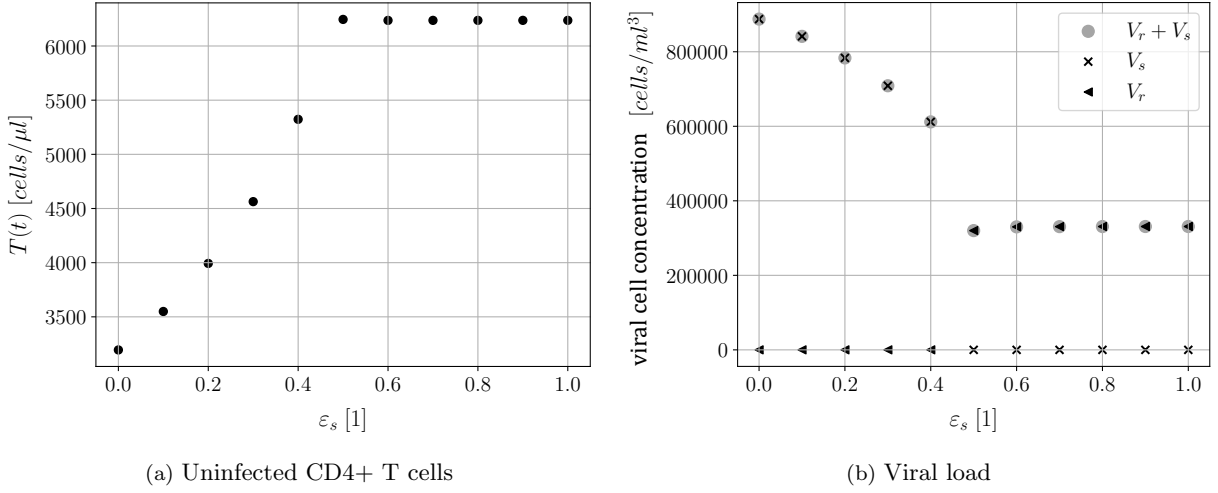


Figure 4: The above diagrams show the dependency of the HIV infection on the drug efficacy parameter ε_s . In the considered case, it is $\varepsilon_{PI}^s = 0$, $\varepsilon_{RT}^s = 0.4$ and $\alpha = 0.2$. Hence, the simulations basically demonstrate the impact of RTIs. Diagram (a) depicts the evolution of the immune cells over increasing ε_s . Diagram (b) shows the same for the concentration of the viral strains. Although, initially enhancing the medication leads to a sinking viral cell count and hence, to a growing CD4+ T concentration, this behaviour changes for a sufficiently high ε_s . Above a certain threshold, the viremia is dominated by drug-resistant HIV cells. The patient does not longer respond to the therapy and her or his count of uninfected immune cells remains constant under increasing ε_s .

In the lower ε_s regime, the total virus count behaves inversely proportional to drug efficacy. For $\varepsilon_{s,max} \leq \varepsilon_s$ this reduction halts after a large drop and the number of free virus settles in a steady state.

An explanation for this behaviour can be found by investigating the evolution of the viral load more closely. While the initial success of the therapy is based on pushing the number of V_s beneath the threshold of detectability, the point of saturation sets in when the concentration of the drug-resistant strain erratically increases. The following consistency of the infection arises from two factors. Firstly, due to the low level of V_s no new mutations emerge. Secondly, RTIs inhibit novel infections of the target cells and hence, the number of drug-resistant virus remains on a stable level. Note, that antiretroviral medications are not in- but only less efficient in attacking drug-resistant viruses. This is included into the model by defining $\varepsilon_{RT}^r = \alpha \varepsilon_{RT}^s$ (as long as $\alpha > 0$).

The quintessence hereof is, that above a certain value $\varepsilon_{s,max}$, simply increasing dose or potency of antiretroviral drugs does not automatically result in an improvement of the therapy but only in an enhancement of their side effects. At the same time, this turning point depends on the model parameters, i.e. on each patient individually. This finding emphasises the necessity to personalize the model.

1.2 The Optimal Control Problem

An optimal therapy is one, that maximizes the level of CD4+ T cells while deploying as few medication as possible. Here, we assume that more and stronger drugs, i.e. higher ε_s and ε_r , are associated with heavier side effects. Further, as shown in the preceding subsection 1.1, above a certain threshold efficacy $\varepsilon_{s,max}$, the effects of HAART saturate.

From mathematical point of view, finding an ideal therapy can be formulated as an optimal control problem. For this, we quantify the cost of HAART in the time interval $[t_0, t_1]$, by the functional

$$J(\varepsilon) = \int_{t_0}^{t_1} (T^2(t) - A_1 \varepsilon_s^2 - A_2 \varepsilon_r^2) dt. \quad (3)$$

The above relation has the following interpretation. The positive effect of the therapy, represented by the number of uninfected CD4+ T cells, is reduced by the negative side-effects of the drugs. This medication burden is quantified by the product of the control parameters $\varepsilon = (\varepsilon_s, \varepsilon_r)^T \in [0, 1]^2$ and their weight constants A_1 and A_2 [1, 6]. Ideally, $T(t)$ is maximised while $A_1 \varepsilon_s^2 + A_2 \varepsilon_r^2$ is minimized. Hence, we seek an optimal control ε_{opt} , such that

$$\varepsilon_{opt} = \arg \max_{\varepsilon \in [0,1]^2} (J(\varepsilon_{opt})). \quad (4)$$

2 The Data

Previously, we have seen that the dynamics of a treated HIV infection is described by a set of nonlinear differential equations. Finding the most efficient HAART while minimizing its side-effects, requires a personalization of the model. This is achieved by estimating the parameters \mathbf{m} from blood measurements. Their acquisition and expected inaccuracies is discussed in this section.

Each new drug therapy is preceded by a preparatory phase during which the total viral cell concentration $V_{tot}(t) = V_r(t) + V_s(t)$ and the CD4+ T cell count $T_{tot}(t) = T(t) + T_r(t) + T_s(t)$ are recorded. In this 8 weeks lasting period, the patient can, obviously, not be left untreated. She or he receives suboptimal therapy, reusing $\varepsilon_{RT}^s = 0.4$ and $\varepsilon_{PI}^s = 0.0$ from above. With $\alpha = 0.2$, it is $\varepsilon_{RT}^r = 0.08$ and $\varepsilon_{PI}^r = 0.0$.

In the previous discussion, we have learned that the initial treatment phase is highly dynamic. Hence, the measurement schedule has to be designed such that the examinations are carried out at intervals, close enough to track these oscillations. At the same time, one wants to make as few blood plasma tests as possible since they are not only time consuming and expensive but also an additional physical and psychological burden for the patient. A good balance is, a one-week interval where once a week, two blood plasma samples are taken. One is used to determine $T_{tot}(t)$, the other for $V_{tot}(t)$.

However, determining the exact amount of virus and immune cells from blood plasma is not trivial. The smallest variations in the sampled plasma volume or too long periods between plasma sampling and final analysis during which viruses can inhibit, are only two factors that potentially contaminate the data with errors. In addition hereto, other aspects such as errors introduced by the laboratory tools, further reduce the reliability of the measurements. Having this in mind, we can interpret the final 8-dimensional observation vectors $\mathbf{T}_{obs} \in \mathbb{R}^8$ and $\mathbf{V}_{obs} \in \mathbb{R}^8$ with $\mathbf{T}_{obs,i} = T_{obs}(t_i)$ and $\mathbf{V}_{obs,i} = V_{obs}(t_i)$, respectively, and for $i \in [0, 7]$, as realizations of random variables. Their statistics are described in terms of the following conditional distributions

$$p(\mathbf{T}_{obs}|\mathbf{m}) = \begin{cases} 0 & T_{obs}(t_i) < 0 \\ \mathcal{N}(\mathbf{T}_{tot}, C_{D_T}) & \text{else} \end{cases}, i \in [0, 7] \quad (5)$$

$$p(\mathbf{V}_{obs}|\mathbf{m}) = \begin{cases} 0 & V_{obs}(t_i) < 0 \\ \mathcal{N}(\mathbf{V}_{tot}, C_{D_V}) & \text{else} \end{cases}, i \in [0, 7] \quad (6)$$

which encode the prior knowledge that we have about the measurements. Firstly, negative cell concentrations are unrealistic and hence, their probability is set to 0. For positive values, we assume that the measurement errors are distributed normally with mean $\mathbf{T}_{tot}(\mathbf{m}) = [T_{tot}(t_0, \mathbf{m}), \dots, T_{tot}(t_7, \mathbf{m})]^T$ and $\mathbf{V}_{tot}(\mathbf{m}) = [V_{tot}(t_0, \mathbf{m}), \dots, V_{tot}(t_7, \mathbf{m})]^T$, respectively. Since single samples are independent of each other, the covariance matrices C_{D_T} and C_{D_V} , have only non-zero diagonal entries. These are the variances in each measurement and describe the observational uncertainty that we have about the value. Determining viral cells in blood plasma is significantly more challenging than tracking the body's own immune cells. This difference is included in the probability distributions by setting $C_{D_V,jj} > C_{D_T,jj}$, $j \in [0, 7]$. We choose $C_{D_T,jj} = 200$ and $C_{D_V,jj} = 250$. Statistics 5 and 6 can further be summarized to describe the joint distribution over all observations, i.e. $p(\mathbf{d}_{obs}|\mathbf{m})$ with $\mathbf{d}_{obs} = \{\mathbf{T}_{obs}, \mathbf{V}_{obs}\}$. Since \mathbf{T}_{obs} and \mathbf{V}_{obs} are derived from independent samples, their joint distribution simplifies to

$$p(\mathbf{d}_{obs}|\mathbf{m}) = p(\mathbf{T}_{obs}, \mathbf{V}_{obs}|\mathbf{m}) = p(\mathbf{T}_{obs}|\mathbf{m})p(\mathbf{V}_{obs}|\mathbf{m}) = \frac{1}{4\pi^2 \sqrt{|C_{D_T}| |C_{D_V}|}} e^{\chi(\mathbf{m})} \quad (7)$$

where $|\cdot|$ is the determinat of a matrix and

$$\begin{aligned} \chi(\mathbf{m}) = & -\frac{1}{2} ((\mathbf{T}_{obs} - \mathbf{T}_{tot}(\mathbf{m}))^T C_{D_T}^{-1} (\mathbf{T}_{obs} - \mathbf{T}_{tot}(\mathbf{m})) \\ & + (\mathbf{V}_{obs} - \mathbf{V}_{tot}(\mathbf{m}))^T C_{D_V}^{-1} (\mathbf{V}_{obs} - \mathbf{V}_{tot}(\mathbf{m}))). \end{aligned} \quad (8)$$

Since we do not have access to real data, we work with artificial data instead. For this, we simulate the means $T_{tot}(t_i)$ and $V_{tot}(t_i)$ by solving the forward model 1 at times $t_i \in \{7i | i \in [0, 7]\}$. Note, that to synthesize the data, we have to predefine the set of true parameters \mathbf{m}_{true} . In the following, we assume that the earlier used values, listed in table 1, are the true parameters which we want to recover from blood measurements.

3 The Methods

After discussing the acquisition of blood measurement data, this section is devoted to consider the model parameters, the inverse problem itself and finally appropriate solution methods in more detail.

3.1 Probabilistic Formulation of Prior Knowledge and Bayes' Theorem

First of all, the aim is to find the model parameters $\mathbf{m} = \{\lambda, \gamma, k_s, k_r, N_s, N_r, \delta, c\} \in \mathbb{R}^8$ which best explain the measured cell loads $\mathbf{d}_{obs} = \{\mathbf{T}_{obs}, \mathbf{V}_{obs}\}$. Generally, the exact values of the parameters are unknown and therefore, are modelled by probability distributions. In doing so, the following prior knowledge can be incorporated. Firstly, from basic physics and biology it can be inferred that the model parameters are always non-negative. Secondly, due to extensive, preceding clinical tests on other HIV patients as well as on animals, the rough order of magnitude of the parameters is known. These prior values are assumed to be the means around which the parameters deviate with a certain variance. Perelson et al. [4], for instance, derive from the infection dynamics that it is reasonable to assume that k_s is uniformly distributed over the interval $(1.2 \times 10^{-8}, 3.6 \times 10^{-8})$ ml day⁻¹. Similar behaviour can be suggested for the drug-resistant population and $k_r \sim \mathcal{U}(1.0 \times 10^{-8}, 3.0 \times 10^{-8})$ ml day⁻¹. Further, the numbers N_s and N_r of viruses that infected CD4+ T cells release after bursting, are again distributed uniformly over (2000, 4000) and (1000, 3000), respectively.

As Rong et al. [5] before, we model the remaining 4 parameters as random variables with an asymmetric triangular distribution. The latter is defined by three values (lb, p, ub) where lb and ub are lower and upper bound, respectively, and p is the peak value. For a random variable x , this statistic is defined as

$$x \sim \mathcal{T}(lb, p, ub) = \begin{cases} \frac{2(x-lb)}{(ub-lb)(p-lb)} & , lb \leq x \leq p \\ \frac{2(ub-x)}{(ub-lb)(ub-p)} & , p < x \leq ub \\ 0 & , x < lb \text{ and } ub < x \end{cases} \quad (9)$$

With that, the death rate γ of uninfected immune cells is drawn from $\mathcal{T}(0.005, 0.01, 0.016)$ day⁻¹. In [5] it is further stated, that the immune cell birth rate λ is a $T(0)$ multiple of γ . Hence, following the discussion from the previous section and using $T(0) = 3.19 \times 10^5$ ml⁻¹, it is $\lambda \sim \mathcal{T}(1.595, 3.19, 5.104) \times 10^4$ ml⁻¹ day⁻¹. The viral clearance rate c is sampled from another asymmetric triangular distribution with lower and upper bounds 9.1 day⁻¹ and 36 day⁻¹, respectively, and peak 23 day⁻¹. Finally, the death rate δ of infected cells is drawn from $\mathcal{T}(0.25, 1, 1.5)$ day⁻¹.

Summarizing the information about the single and mutually independent model parameters, their joint probability distribution takes the form

$$p(\mathbf{m}) = p(\lambda)p(\gamma)p(k_s)p(k_r)p(N_s)p(N_r)p(\delta)p(c). \quad (10)$$

After representing the prior knowledge in data and model space in form of probability distributions, the next step can be taken and the inverse problem itself is considered. First of all, the problem, with its eight unknown model parameters $\mathbf{m} \in \mathbb{R}^8$, and the eight observations $\mathbf{d}_{obs} \in \mathbb{R}^8$ is even-determined. In section 2, it has been mentioned that *as few as possible* blood plasma test should be conducted. Here, the minimal number is set by the necessity to generate at least as many observations as unknown parameters in order to avoid an over- or under-determined problem.

Following this, the inverse problem has to be formulated. Generally, there are three possibilities namely defining the inversion as an optimization problem, a deterministic least-squares problem or a Bayesian inverse problem. The first option is based on approximating a problem-dependent misfit function. This approach is appropriate for a weakly non-linear forward problem. Opposed to that, a deterministic least-square problem solves the root-mean square misfit function for a linear forward model. Since this includes the inversion of possibly singular matrices, one has to incorporate prior knowledge as well as regularization techniques (equivalent to include artificial prior knowledge). Last but not least, a Bayesian inverse problem derives the a posteriori model

distribution $p(\mathbf{m}|\mathbf{d}_{obs})$ from the prior distributions in model and data space with Bayes theorem. Following this, computationally expensive Monte Carlos Methods are used to sample from the posterior distribution since the latter is generally not given explicitly. The finally selected model is then for instance the *maximum a posterior model* \mathbf{m}_{MAP} . In a special case, where the forward model is linear and both prior distributions are Gaussian, the probabilistic approach of Bayes can be formulated as a least-squares problem and the posterior distribution can be defined explicitly.

However, the fact that the forward model for the HIV dynamics is non-linear and none of the prior distributions is purely Gaussian, directly excludes the least-square approach. Further, one could either choose to linearize the forward model and define the problem as an optimization or to formulate it as a Bayes inverse problem. An often mentioned disadvantages of the latter is, that sampling from a distribution with Monte Carlo Methods is computationally expensive. Apart from that, Bayes approach has no inherent limitation and even has the strong advantage to directly include an uncertainty quantification since the likelihood is directly attached to each model as a measure of plausibility.

Hence, despite the high computational cost, it is reasonable to formulate the problem as a Bayes inversion. It is

$$p(\mathbf{m}|\mathbf{d}_{obs}) = \frac{p(\mathbf{d}_{obs}|\mathbf{m})p(\mathbf{m})}{p(\mathbf{d}_{obs})} . \quad (11)$$

where we aim on computing the maximum likelihood estimation of $p(\mathbf{m}|\mathbf{d}_{obs})$.

3.2 Sampling with Markov Chain Monte Carlo Method

As mentioned above, in most cases the posterior model distribution $p(\mathbf{m}|\mathbf{d}_{obs})$ can not be computed analytically and hence, Bayes approach has to be equipped with an algorithm to sample from it. A very simple choice would be a systematic grid search in the model space. However, since it heavily suffers from the curse of dimensionality, Monte Carlo Methods (MCM) are more appropriate. Generally speaking, these methods are capable of numerically solving a broad class of computational problems by repeated random sampling. Here, we use MCM to compute samples of the model posterior distribution. For this, a Markov Chain is constructed whose equilibrium distribution equals $p(\mathbf{m}|\mathbf{d}_{obs})$. The arising class of algorithms are called Markov Chain Monte Carlo (MCMC) methods. While simple grid searches deterministically scan through the complete model space, MCMC perform random searches. They try to avoid regions in the search space that are less relevant than other. Meaningful models are identified by taking the prior knowledge into account.

A special MCMC algorithm is the so-called Simulated Annealing (SA). Based on the Metropolis-Hasting acceptance rule, it samples from a modified posterior probability distribution $p_T(\mathbf{m}|\mathbf{d}_{obs})$. Due to this modification of the distribution, the algorithm starts sampling from a very broad $p_T(\mathbf{m}|\mathbf{d}_{obs})$. In the course of the SA sampling, the peaks of the modified distribution become more and more distinct. For a sufficiently slow transition from the broad $p_T(\mathbf{m}|\mathbf{d}_{obs})$ to the distinct one, convergence towards the global maximum-likelihood model is guaranteed.

Hence, the solution of the inverse problem is automatically the maximum likelihood model \mathbf{m}_{MAP} . As mentioned earlier, Bayes approach does not require any additional uncertainty assessment.

References

- [1] B. M. Adams, H. T. Banks, M. Davidian, H.-D. Kwon, H. T. Tran, S. N. Wynne, and E. S. Rosenberg. Hiv dynamics: modeling, data analysis, and optimal treatment protocols. *Journal of Computational and Applied Mathematics*, 184(1):10–49, 2005.
- [2] R. M. Anderson. Complex dynamic behaviours in the interaction between parasite populations and the host’s immune system. *International journal for parasitology*, 28(4):551–566, 1998.
- [3] A. S. Perelson, D. E. Kirschner, and R. De Boer. Dynamics of hiv infection of cd4+ t cells. *Mathematical biosciences*, 114(1):81–125, 1993.
- [4] A. S. Perelson, D. E. Kirschner, and R. De Boer. Dynamics of hiv infection of cd4+ t cells. *Mathematical Biosciences*, 114(1):81 – 125, 1993.
- [5] L. Rong, Z. Feng, and A. S. Perelson. Emergence of hiv-1 drug resistance during antiretroviral treatment. *Bulletin of Mathematical Biology*, 69(6):2027–2060, 2007.
- [6] J. Wu and M. Zhang. A game theoretical approach to optimal control of dual drug delivery for hiv infection treatment. *IEEE Transactions on Systems, Man, and Cybernetics, Part B (Cybernetics)*, 40(3):694–702, 2010.